Bond disorder, frustration and polymorphism
in the spontaneous crystallization of a polymer melt

A. Giuntoli

Dipartimento di Fisica "Enrico Fermi", Università di Pisa, Largo B.Pontecorvo 3, I-56127 Pisa, Italy

S. Bernini

Dipartimento di Fisica "Enrico Fermi", Università di Pisa, Largo B.Pontecorvo 3, I-56127 Pisa, Italy

D. Leporini*

Dipartimento di Fisica "Enrico Fermi", Università di Pisa, Largo B.Pontecorvo 3, I-56127 Pisa, Italy

IPCF-CNR, UOS Pisa, Italy

Abstract

The isothermal, isobaric spontaneous crystallization of a supercooled polymer melt is investigated by MD simulation of an ensemble of fully-flexible linear chains. Frustration is introduced via two incommensurate length scales set by the bond length and the position of the minimum of the non-bonding potential. Marked polymorphism with considerable bond disorder, distortions of both the local packing and the global monomer arrangements is observed. The analyses in terms of: i) orientational order parameters characterizing the global and the local order and ii) the angular distribution of the next-nearest neighbors of a monomer reach the conclusion that the polymorphs are arranged in distorted Bcc-like lattices.

1. Introduction

Crystallization plays an important role in many areas of different scientific fields, ranging from biology to engineering and physics. Still, many microscopic details of the phenomenon are unknown, despite the abundance of related results both experimental and theoretical [1–11]. In particular, polymeric liquids are systems in which the structural features, namely the chain connectivity, cause serious hindrance to the homogeneous crystallization of the sample. In silico simulations of such systems provide great insight on this problem and have proven to be an invaluable tool in the analysis of the crystallization under controlled conditions [3]. Many simulations have been performed aiming at observing the crystallization of polymers and characterizing the structural order reached by the crystalline

sample under various conditions [12–20]. Recently, Monte Carlo (MC) simulations of polymer melts made by linear chains of tangent hard-sphere monomers [21–23], i.e. with bond length *equal* to monomer diameter, have been performed to study spontaneous crystallization. The resulting crystallized structures have been interpreted as a distribution of the most densely packed structures: face-centered cubic (Fcc) and hexagonal close packed (Hcp) lattices. Hcp and Fcc were selected as ideally ordered structures because they are known to be the primary competing alternatives in dense systems of hard spheres in the presence of a single length scale [21]. MC simulations, differently from Molecular Dynamics (MD) simulations, may fail to account for the arrest into metastable intermediate phases [22] which hinder the evolution towards the thermodynamically stable phase [24]. MD simulations of a polymer melt of chains with soft monomers, promoting the crystallization by equal bond length and equilibrium nonbonded separation, have been performed with the aim of comparing the crystalline structures obtained by cooling down to zero temperature with the highly packed

---

Fcc and Hcp lattices [25, 26]. Still, the route towards the closest packing of polymers is hindered by allowing length-scale competition of the bonding and the non-bonding interactions, as recently proven in a MD study of the crystallization triggered by confinement due to Fcc walls, where structures similar to body-centered cubic (Bcc) are observed [27].

Polymorphism, the presence of different crystal structures of the same molecule, is a well-known phenomenon in molecular crystals [28]. In particle systems the crystal structure depends on the steepness of the repulsive part of the interacting potential with hard and soft repulsions favoring Fcc and Bcc ordering respectively [29]. To date, the selection mechanism of polymorphs is elusive. One widely used criterion is the Ostwald step rule, stating that in the course of transformation of an unstable, or metastable state, into a stable one the system does not go directly to the most stable conformation but prefers to reach intermediate stages having the closest free energy to the initial state [24, 28, 30, 31]. Alternatives are reported [32].

In this work the isothermal *spontaneous* crystallization of an unbounded polymeric system is studied via MD simulation of *fully-flexible* linear chains, i.e. bond-bending and bond-torsions potentials are not present. The emphasis is on the global and local order of the crystalline phase with respect to the pristine super-cooled liquid where crystallization started. To this aim, specific order parameters will be used for their characterization [33, 34]. A distinctive feature of the model is the presence of two *different* length scales, namely the bond length b and the distance σ^* where the minimum of the non-bonding potential, the Lennard-Jones (LJ) pair potential, is located. It is known that the competition of two incommensurate length scales favors frustration in the self-assembly of ordered structures from an initial disordered state, like in molecular crystallization [35]. Frustrated crystallization of polymers has been reviewed [36]. The role played in the crystallization behavior (including its absence) by frustration, where there is an incompatibility between the preferred local order and the global crystalline order, has been highlighted [37]. We expect different responses to frustration from the putative crystalline structures at finite temperature, i.e. Fcc, Hcp and Bcc lattices. In fact, not all the atoms in the first neighbors shell of a Bcc lattice are at the same distance, as in the Fcc and Hcp lattices. It is known that the mechanical stability of the Bcc structure is lower than in closed packed structures as Fcc [29].

The paper is organized as follows: In Sec.2 the polymer model is detailed and the simulation details are provided. The results are presented and discussed in Sec.3.

Finally, the conclusions are drawn in Sec.4.

2. Methods

We consider a coarse-grained polymer model of $N_c = 50$ linear, unentangled chains with $M = 10$ monomers per chain. The total number of monomers is $N = 500$. The chains are fully-flexible, i.e. bond-bending and bond-torsions potentials are not present. Non-bonded monomers at distance r interact via the truncated Lennard-Jones (LJ) potential:

$$U^{LJ}(r) = \varepsilon \left[\left(\frac{\sigma^*}{r} \right)^{12} - 2 \left(\frac{\sigma^*}{r} \right)^6 \right] + U_{cut} \quad (1)$$

for $r \leq r_c = 2.5\,\sigma$ and zero otherwise, where $\sigma^* = 2^{1/6}\sigma$ is the position of the potential minimum with depth ε. The value of the constant U_{cut} is chosen to ensure that $U^{LJ}(r)$ is continuous at $r = r_c$. Henceforth, all quantities are expressed in terms of reduced units: lengths in units of σ, temperatures in units of ε/k_B (with k_B the Boltzmann constant) and time τ_{MD} in units of $\sigma\sqrt{m/\varepsilon}$ where m is the monomer mass. We set $m = k_B = 1$. The bonding interaction is described by an harmonic potential U^b [38]:

$$U^b(r) = k(r - r_0)^2 \quad (2)$$

The parameters k and r_0 have been set to $2500\,\varepsilon/\sigma^2$ and $0.97\,\sigma$ respectively [39]. Given the high stiffness of the bonding interaction, $b = 0.97 \pm 0.02$. Notice that the bond length and the minimum of the non-bonding potential are *different*, $b \neq \sigma^* \simeq 1.12$. Periodic boundary conditions are used. The study was performed in the NPT ensemble (constant number of particles, pressure and temperature). The integration time step is set to $\Delta t = 0.003$ time units [40–45]. The simulations were carried out using LAMMPS molecular dynamics software (http://lammps.sandia.gov) [46]. The samples were initially equilibrated at temperature $T = 0.7$ and pressure $P = 4.7$ for a lapse of time which is, at least, three times the average reorientation time of the end-end vector of the chain [47]. After equilibration, we started production runs waiting for the spontaneous crystallization of the system. We analyzed the initial equilibrated liquid state, the development of the solid phase and the final crystalline state. 56 starting configurations of the liquid were used with different random velocities, chain conformations and non-overlapping monomer positions. 42 equilibrated runs underwent crystallization, while 14 of them failed to crystallize in a reasonable amount of time (about one month of computing time).
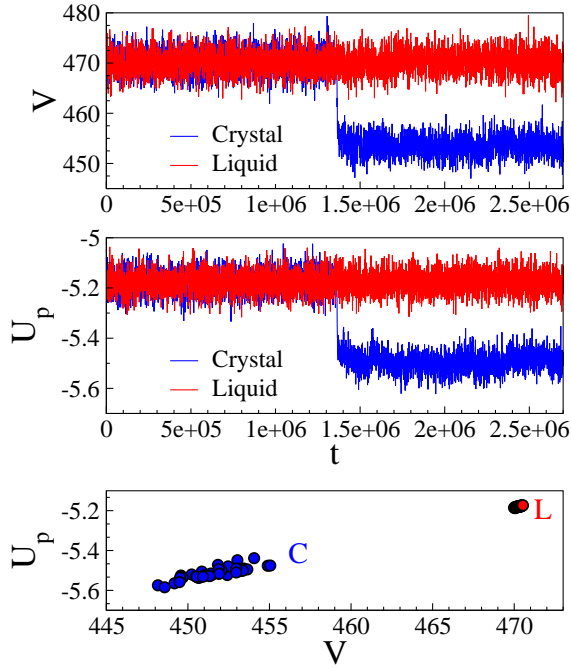
Figure 1: Volume (top) and potential energy (middle) drops due to the spontaneous crystallization occurring in a single run (blue curve). They are compared to the typical fluctuations occurring in the metastable liquid (red curve). The bottom panel is a correlation plot between the average volume and the energy of all the crystalline (blue) and liquid (red) states under study. Note the large region spanned by the different crystalline states signaling polymorphism.

3. Results and discussion

The spontaneous crystallization of the polymeric system is characterized by a sudden drop of both the volume V and the potential energy U_p during the time evolution of the system, as shown in Fig.1. It is seen that the mean values of both the volume and the potential energy of the crystals span a wider range with respect to the the metastable liquid, see lower panel of Fig.1. This is evidence of polymorphism due to different kinetic pathways leading to crystallization in more than one, metastable, ordered form [28]. In our polymer melt polymorphism is contributed, with respect to the corresponding - non-bonded - atomic liquid, by the chain connectivity and the presence of incommensurate length scales involving the bonding and the non-bonding potentials.

In order to start the characterization of the polymorphism, we consider the arrangements of both the monomer and the bonds by the radial distribution function $g(r)$ and the distribution $P(\cos\theta)$ of the angle θ between adjacent bonds in a chain, respectively. The re-
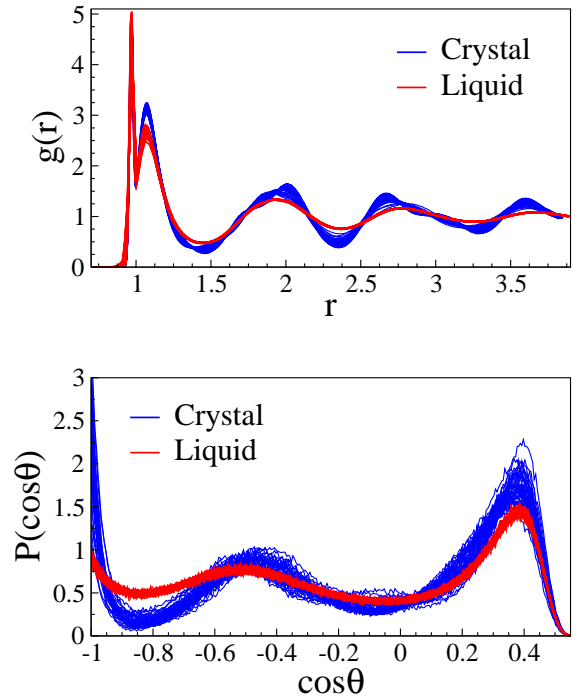

Figure 2: Top: radial pair distribution function $g(r)$ of all the crystalline and liquid states. On increasing the distance r from the tagged central monomer, the first, sharp peak corresponds to the bonded monomers, whereas the other ones signal the different neighbor shells. Bottom: distribution $P(\cos\theta)$ of the angle θ between adjacent bonds in a chain. The peaks occur at $\theta \approx 70°, 122°, 180°$, corresponding to three consecutive monomers which are folded - with the two non-consecutive monomers in contact ($r \sim \sigma^*$) -, partially folded, and aligned, respectively [34]. Notice that the broad features of both $g(r)$ and $P(cos\theta)$ of the crystalline and the melt states are quite similar. Nonetheless, the ordered states exhibit sharper and, due to polymorphism, more widely distributed features than the disordered ones.

sults are reported in Fig.2 and are compared to the corresponding ones of the liquid. It is apparent that $g(r)$ and $P(\cos\theta)$ are not markedly different in the polymorph and the liquid states even if the polymorphs exhibit sharper, and more widely distributed, features, including a larger fraction of aligned bonds.

The description of the selection mechanism of the polymorph is beyond the purpose of the present work. As initial step, we study the monomer mobility during the transition from the liquid to the polymorph. To this aim, we resort to the self-part of the van Hove function $G_s(r,t)$ [48]. The product $G_s(r,t) \cdot 4\pi r^2$ is the probability that the monomer is at a distance between r and $r + dr$ from the initial position after a time t. We observe that the crystallization completes in a range of times spanning from about $0.8 \cdot 10^4$ up to $1.5 \cdot 10^4$ MD times for the different runs. The average value of
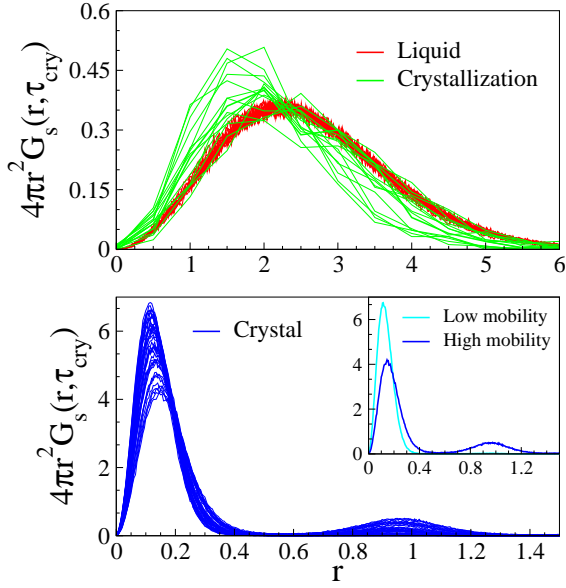
Figure 3: Displacement distribution of the monomers in a time τ_{cry} during different stages of the crystallization. The average time to start and complete the crystallization is $\tau_{cry} = 12000$. Top: initial super-cooled liquids in metastable equilibrium (red), selected supercooled liquid states undergoing crystallization (green). Different curves with same color refer to different crystallization paths. Bottom: final poly-morphs. The small peak at $r \sim 1$ signals the presence of monomers jumping of about one diameter. The initial liquid state of the paths ex-hibits always nearly the same displacement distribution. The displace-ment distribution during the crystallization process is only mildly nar-rower than the one of the melt. The different polymorphs have distinct displacement distributions and lower mobility than the liquid. The in-set of the bottom panel shows the two polymorphs with highest and lowest mobility, respectively. The jump process is largely suppressed in the less mobile polymorph.

the crystallization time is $\tau_{cry} = (1.2 \pm 0.1) \cdot 10^4$ time units, corresponding to 22 ± 2 ns mapping the MD units on polyethylene, according to the procedure outlined in ref. [49]. Notice that the MD-polyethylene conversion factor, $\sigma\sqrt{m/\varepsilon} = 1.8$ ps, is in the range usually found for polymers, i.e. $\sim 1 - 10$ ps/ MD time step [49]. Our average crystallization time is intermediate between the induction time, i.e. the average time to reach the crit-ical nucleus size and proceed with further growth at later times [50], of n-octane, 16 ± 10 ns [51], and n-eicosane , 80.6 ± 8.8 ns [52], as evaluated by using a realistic, united-atom MD model for n-alkanes. No clear correlation between the crystallization time and crystal type was observed. For the different crystalliza-tion paths we evaluate the displacement distribution in a time τ_{cry} of: i) the initial liquid in metastable equi-librium, ii) the liquid during crystallization and iii) the final polymorph. The results are in Fig.3. During the
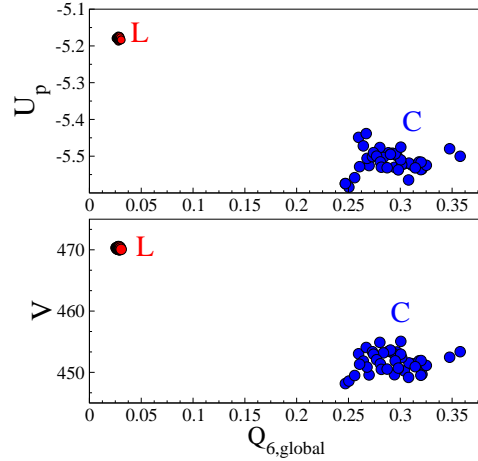

Figure 4: Correlation plot between the global order parameter $Q_{6,global}$ and both the potential energy (top) and volume (bottom). Both liquid states (red) and polymorphs (blue) are shown. Poly-morphs span an extended region of the plot with larger global order than the liquid.

crystallization monomers displace nearly as far as in the liquid. Starting from liquid states with nearly identical displacement distribution, see Fig.3 (top), each subse-quent crystallization path and final polymorph is char-acterized by a different displacement distribution. Poly-morphs have little mobility. Their displacement distri-bution exhibits a bimodal structure with a large peak corresponding to the rattling motion of the monomer within the cage of the first neighbors and a secondary peak due to monomers displacing by jumps with size comparable to their diameter. The inset of Fig.3 shows the displacement distribution of the polymorphs with the highest and the lowest mobility and evidences that the jump process is largely suppressed in the less mobile polymorph.

In order to study more rigorously the structural order of the system, we resort to the order parameters defined by Steinhardt *et al.* [33]. One considers in a given coor-dinate system the polar and azimuthal angles $\theta(\mathbf{r}_{ij})$ and $\phi(\mathbf{r}_{ij})$ of the vector $\mathbf{r}_{ij}$ joining the i-th central monomer with the j-th one belonging to the neighbors within a preset cutoff distance $r_{cut} = 1.2\ \sigma^* \simeq 1.35$ [33]. r_{cut} is a convenient definition of the first coordination shell size [53]. The vector $\mathbf{r}_{ij}$ is usually referred to as a "bond" and has not to be confused with the *actual* chem-ical bonds of the polymeric chain. To define a global measure of the order in the system, one then introduces
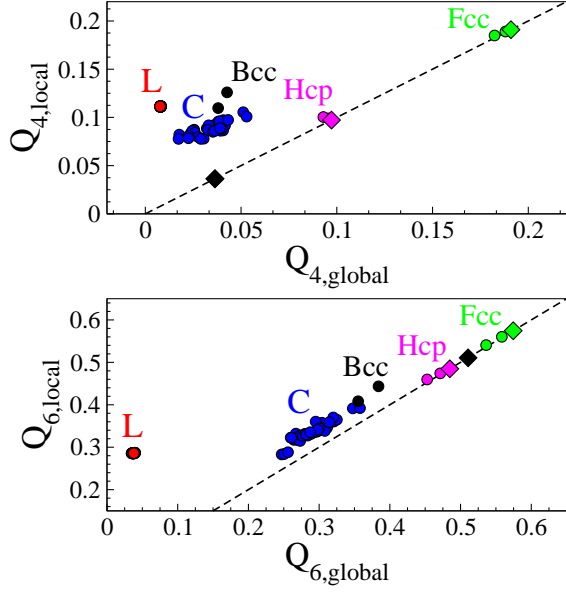
Figure 5: Correlation plots between the local and the global parameters with $l = 4$ (top) and $l = 6$ (bottom) for polymorphs (blue dots) and liquids (red dots). The dashed line is the bisectrix. The diamonds mark the ideal Bcc- (black), Fcc- (green) and Hcp- (magenta) atomic crystals at T=0 with $Q_{l,global} = Q_{l,local}$. The black, green and magenta dots mark the same crystals at $T = 0.3, 0.7$. Differently from the Bcc lattice, the global and the local order of the Fcc and Hcp lattices are negligibly affected by the temperature, signaling more thermal stability. In each plot the black dot closest to the polymorph region is the Bcc lattice at the same temperature ($T = 0.7$).
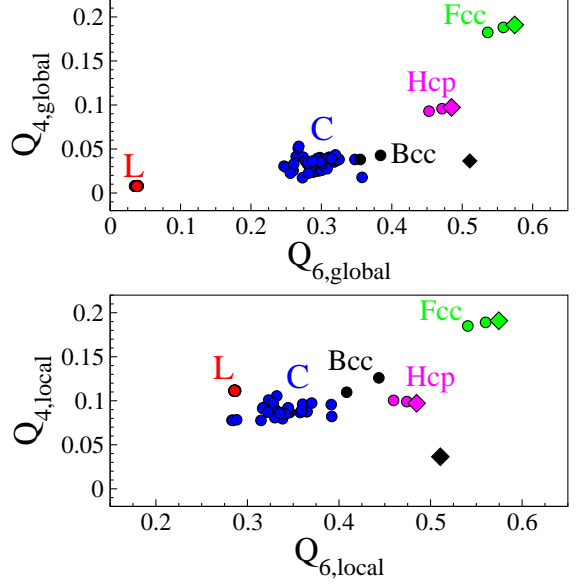
Figure 6: Correlation plots $Q_{4,global}$ vs. $Q_{6,global}$ (top) and $Q_{4,local}$ vs. $Q_{6,local}$ (bottom). All the symbols are used as in Fig.5. In each plot the black dot closest to the polymorph region is the Bcc lattice at the same temperature ($T = 0.7$).

the quantity:

$$\bar{Q}_{lm}^{global} = \frac{1}{N_b} \sum_{i=1}^{N} \sum_{j=1}^{n_b(i)} Y_{lm} \left[\theta(\mathbf{r}_{ij}), \phi(\mathbf{r}_{ij}) \right] \quad (3)$$

where $n_b(i)$ is the number of bonds of i-th particle, N is the total number of particles in the system, Y_{lm} denotes a spherical harmonic and N_b is the total number of bonds:

$$N_b = \sum_{i=1}^{N} n_b(i) \quad (4)$$

The global orientational order parameter $Q_{l,global}$ is defined by:

$$Q_{l,global} = \left[\frac{4\pi}{(2l+1)} \sum_{m=-l}^{l} |\bar{Q}_{lm}^{global}|^2 \right]^{1/2} \quad (5)$$

The above quantity is invariant under rotations of the coordinate system and takes characteristic values which can be used to quantify the kind and the degree of rotational symmetry in the system [33]. In the absence of *large*-scale order, the bond orientation is uniformly distributed around the unit sphere and $Q_{l,global}$ is rather small since it vanishes as $\sim N_b^{-1/2}$ [54]. On the other hand, $Q_{6,global}$ is very sensitive to any kind of crystallization and increases significantly when order appears [55]. A local orientational parameter $Q_{l,local}$ can also be defined. We define the auxiliary quantity

$$\bar{Q}_{lm}^{local}(i) = \frac{1}{n_b(i)} \sum_{j=1}^{n_b(i)} Y_{lm} \left[\theta(\mathbf{r}_{ij}), \phi(\mathbf{r}_{ij}) \right] \quad (6)$$

The local order parameter $Q_{l,local}$ is defined as [33]:

$$Q_{l,local} = \frac{1}{N} \sum_{i=1}^{N} \left[\frac{4\pi}{(2l+1)} \sum_{m=-l}^{l} |\bar{Q}_{lm}^{local}(i)|^2 \right]^{1/2} \quad (7)$$

In general $Q_{l,local} \geq Q_{l,global}$. In the presence of ideal order, *all* the particles have the *same* neighborhood configuration, and the equality $Q_{l,local} = Q_{l,global} = Q_l$ follows.

Fig.4 shows the correlations between the volume V, the potential energy U_p and the global order parameter $Q_{6,global}$ for both the liquids and the polymorphs. We see that liquid states have rather small $Q_{6,global}$ with narrow distributions of V, U_p and $Q_{6,global}$. The polymorphs have much larger $Q_{6,global}$ values with wider distributions of V, U_p and $Q_{6,global}$.
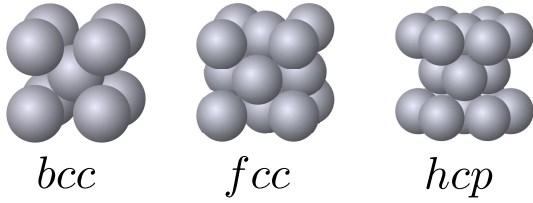
Figure 7: Bcc-, Fcc- and Hcp-lattices at $T = 0$. Fcc and Hcp structures are closely packed and each atom is surrounded by twelve neighbors at the distance a. In the Bcc structure each atom has neighbors at two different distances: a and $2a/\sqrt{3}$.

An interesting features of the order parameters is that they exhibit specific values for the different kind of orders [33]. This suggests to plot their values to gain insight into the global and the local order of the polymorphs and the liquid. This is done in Fig.5 and Fig.6. First, let us refer to Fig.5 providing correlation plots $Q_{l,global}$ vs $Q_{l,local}$ for $l = 4, 6$. We see that $Q_{l,global}$ is higher in the polymorphs than in the liquids, whereas $Q_{l,local}$ is nearly the same. In order to better understand the results, we added to Fig.5 the Bcc, Fcc and Hcp crystals at different temperatures as reference crystals. In the reference crystals atoms interact via the LJ potential. At $T = 0$ the closest particles are spaced by the average monomer-monomer distance of the polymer system, $a = 1.07$. Their structure is shown in Fig.7. Bcc, Fcc and Hcp crystals at $T = 0$ are characterized by the equality $Q_{l,global} = Q_{l,local}$. We also included the same atomic crystals at $T = 0.3, 0.7$. Fig.5 shows that, when increasing the temperature, the order parameters of both Fcc and Hcp atomic lattices show little changes, whereas the ones of the Bcc crystal are much more sensitive. This is consistent with the known lower stability of the Bcc crystal [29]. Fig.5, especially the case with $l = 6$ (bottom panel), shows that the polymorphs position themselves in an region close to the one of the Bcc structure at the same temperature ($T = 0.7$). This is a piece of evidence that our melt of fully-flexible chains crystallizes spontaneously into a Bcc-like structure distorted by the polymer connectivity. Fig.6 presents different pairs of order parameters. It is seen that the pair of global parameters (top panel) are more informative and confirm the conclusions drawn by the analysis of Fig.5, i.e. the structures of the polymorphs approach the one of the Bcc structure at the same temperature ($T = 0.7$).

Further support to the conclusion that fully-flexible chains crystallize in a Bcc-like structure is provided by the angular distribution of the monomers belong-
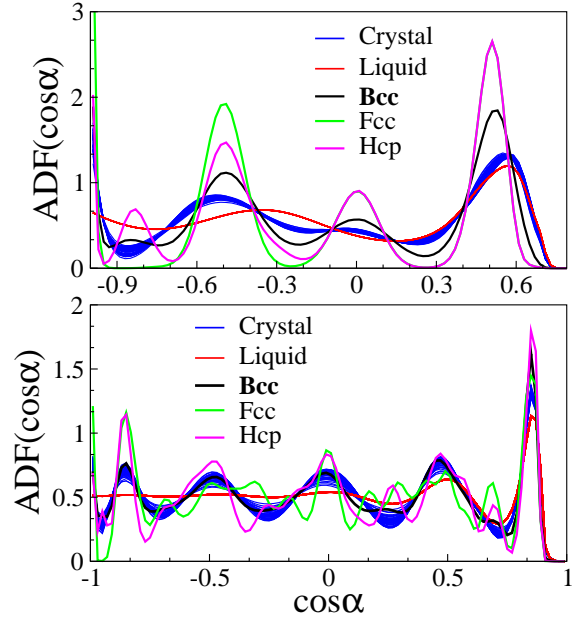

Figure 8: Angular distribution function (ADF) in the first ($0.8 < r < 1.35$, top panel) and second ($1.35 < r < 2.2$, bottom panel) shells of the liquids and the polymorphs. As reference, the distributions of Bcc, Fcc and Hcp crystals at $T = 0.7$ are also plotted. Different polymorphs exhibit distinct ADFs. No clear conclusion is drawn by comparing the ADF of the crystalline polymers and the ones of the atomic Bcc, Fcc and Hcp crystals in the first shell. Instead, the ADF of the crystalline polymers and the Bcc crystal at $T = 0.7$ is almost identical in the second shell.

ing to specific shells of neighbors surrounding a central monomer. To this aim, we modify the Steinhardt procedure and consider the angle α_{jk} between $\mathbf{r}_{ij}$ and $\mathbf{r}_{ik}$ where the vector $\mathbf{r}_{ij}$ joins the i-th central monomer with the j-th one which is r_{ij} apart. Our quantity of interest is the angular distribution function $ADF(\cos \alpha_{jk})$ of the monomers with $r_{min} \leq r_{ij}, r_{ik} \leq r_{max}$. Fig.8 shows the ADF distribution for the polymorphs and the liquids restricted to the first and the second shells, respectively. As a reference, the ADF distributions of Bcc, Fcc and Hcp crystals at $T = 0.7$ are also plotted. On the basis of the radial distribution function in Fig.2 (top), the boundaries of the shells are taken as: $r_{min} = 0.8$, $r_{max} = 1.35$ (first shell) and $r_{min} = 1.35, r_{max} = 2.2$ (second shell). It is seen that the ADF distributions of the different polymorphs are distinct. They differ from both the liquid and the reference atomic crystals in the first shell. Differently, the ADF distributions of the different polymorphs are in excellent agreement with the Bcc ADF in the *second* shell. It is worth noting that the ADF of the liquid is nearly flat in the second shell for $\cos \alpha < 0$, signaling the large loss of anisotropy beyond

the first shell.

4. Conclusions

The isothermal, isobaric spontaneous crystallization of a supercooled polymer melt is investigated by MD simulation of an ensemble of fully-flexible linear chains. Frustration is introduced via two incommensurate length scales, i.e. the bond length and the minimum of the non-bonding potential, resulting in marked polymorphism with considerable bond disorder, distortions of both the local packing and the global monomer arrangements. The crystallization process involves monomer displacements as large as a few diameters. Jump processes are detected in the polymorphs. The analyses in terms of: i) orientational order parameters characterizing the global and the local order and ii) the angular distribution of the next-nearest neighbors of a monomer reach the conclusion that the polymorphs are arranged in distorted Bcc-like lattices.

Acknowledgements

References

[1] P. J. Phillips, Polymer crystals, Rep. Prog. Phys. (1990) 549–604.

[2] B. G. Sumpter, D. W. Noid, B. Wunderlich, Computer experiments on the internal dynamics of crystalline polyethylene: Mechanistic details of conformational disorder, J. Chem. Phys. 93 (1990) 6875.

[3] N. C. Karayiannis, K. Foteinopoulou, M. Laso, Spontaneous crystallization in athermal polymer packings, Int. J. Mol. Sci. 14 (2013) 332–358.

[4] J. Russo, H. Tanaka, The microscopic pathway to crystallization in supercooled liquids, Sci. Rep. 2 (2012) 00505.

[5] M. Leomach, H. Tanaka, Roles of icosahedral and crystal-like order in the hard spheres glass transition, Nat. Commun. 3 (2012) 974.

[6] M. R. Jones, R. J. Macfarlane, B. Lee, J. Zhang, K. L. Young, A. J. Senesi, C. A. Mirkin, Dna-nanoparticle superlattices formed from anisotropic building blocks, Nat. Mater. 9 (2010) 913–917.

[7] D. Nykypanchuk, M. M. Maye, D. Leile, O. Gang, Dna-guided crystallization of colloidal nanoparticles, Nature 451 (2008) 549–552.

[8] D. J. Gundlach, J. E. Royer, S. K. Park, S. Subramanian, O. D. Jurchescu, B. H. Hamadani, A. J. Moad, R. J. Kline, L. C. Teague, O. Kirillov, C. A. Richter, J. G. K. L. J. Richter, S. R. Parkin, T. N. Jackson, J. E. Anthony, Contact-induced crystallinity for high-performance soluble acene-based transistors and circuits, Nat. Mater. 7 (2008) 216–221.

[9] M. Campoy-Quiles, T. Ferenczi, T. Agostinelli, P. G. Etchegoin, Y. Kim, T. D. Anthopoulos, P. N. Stavrinou, D. D. C. Bradley, J. Nelson, Morphology evolution via self-organization and lateral and vertical diffusion in polymer: fullerene solar cell blends, Nat. Mater. 7 (2008) 158–164.

[10] J. Hegedüs, S. R. Elliott, Microscopic origin of the fast crystallization ability of Ge-Sb-Te phase-change memory materials, Nat. Mater. 7 (2008) 399–405.

[11] Y. Loo, R. A. Register, A. J. Ryan, G. T. Dee, Polymer crystallization confined in one, two, or three dimensions, Macromolecules 34 (2001) 8968–8977.

[12] M. Tanemura, Y. Hiwatari, H. Matsuda, T. Ogawa, N. Ogita, A. Ueda, Geometrical analysis of crystallization of the soft-core model, Progr. Theor. Phys. 58 (1977) 1079–1095.

[13] J. Hahn, J. Pertsin, , H. P. Grossmann, Monte-carlo simulation of solid-solid transition to conformationally disordered state, Macromolecules 25 (1992) 6510–6515.

[14] V. Trappe, V. Prasad, L. Cipelletti, P. N. Segre, D. A. Weitz, Jamming phase diagram for attractive particles, Nature 411 (2001) 772–775.

[15] H. Meyer, F. Müller-Plathe, Formation of chain-folded structures in supercooled polymer melts examined by MD simulations, Macromolecules 35 (2002) 1241–1252.

[16] Z. H. Stachurski, Definition and properties of ideal amorphous solids, Phys. Rev. Lett. 90 (2003) 155502.

[17] A. V. Anikeenko, N. N. Medvedev, Structural and entropic insights into the nature of the random-close-packing limit, Phys. Rev. E 77 (2008) 031101.

[18] A. Ikeda, L. Berthier, P. Sollich, Unified study of glass and jamming rheology in soft particle systems, Phys. Rev. Lett. 109 (2012) 018301.

[19] R. Ni, M. Dijkstra, Effect of bond length fluctuations on crystal nucleation of hard bead chains, Soft Matter 9 (2012) 365–369.

[20] L. M. Lopatina, O. Reichhardt, C. Reichhardt, Jamming in granular polymers, Phys. Rev. E 84 (2014) 011303.

[21] N. C. Karayiannis, K. Foteinopoulou, M. Laso, The characteristic crystallographic element norm: A descriptor of local structure in atomistic and particulate systems, J. Chem. Phys. 130 (2009) 074704.

[22] N. C. Karayiannis, K. Foteinopoulou, M. Laso, Entropy-driven crystallization in dense systems of athermal chain molecules, Phys. Rev. Lett. 103 (2009) 045703.

[23] N. C. Karayiannis, K. Foteinopoulo, C. F. Abrams, M. Laso, Modeling of crystal nucleation and growth in athermal polymers: self-assembly of layered nano-morphologies, Soft Matter 6 (2010) 2160–2173.

[24] P. R. ten Wolde, D. Frenkel, Homogeneous nucleation and the ostwald step rule, Phys. Chem. Chem. Phys. 1 (1999) 2191–2196.

[25] R. S. Hoy, N. C. Karayiannis, Simple model for chain packing and crystallization of soft colloidal polymers, Phys. Rev. E 88 (2013) 012601.

[26] H. T. Nguyen, T. B. Smith, R. S. Hoy, N. C. Karayiannis, Effect of chain stiffness on the competition between crystallization and glass-formation in model unentangled polymers, J. Chem. Phys. 143 (2015) 144901.

[27] M. E. Mackura, D. S. Simmons, Enhancing heterogeneous crystallization resistance in a bead-spring polymer model by modifying bond length, J. Polym. Sci. Part B: Polym. Phys. 52 (2014) 134–140.

[28] J. Bernstein, Polymorphism in Molecular Crystals, Clarendon Press, Oxford, 2002.

[29] F. Milstein, Mechanical stability of crystal lattices with two-body interactions, Phys. Rev. B 2 (1970) 512–518.

[30] W. F. Ostwald, Studien über die bildung und umwandlung fester

körper. studies on formation and transformation of solid materials., Z. Phys. Chem. 22 (1897) 289–330.

[31] L. Larini, D. Leporini, A manifestation of the ostwald step rule: Molecular-dynamics simulations and free-energy landscape of the primary nucleation and melting of single-molecule polyethylene in dilute solution, J. Chem. Phys. 123 (2005) 144907.

[32] J. Russo, H. Tanaka, Selection mechanism of polymorphs in the crystal nucleation of the gaussian core model, Soft Matter 8 (2012) 4206–4215.

[33] P. J. Steinhardt, D. R. Nelson, M. Ronchetti, Bond-orientational order in liquids and glasses, Phys. Rev. B 28 (1983) 784–805.

[34] S. Bernini, F. Puosi, M. Barucco, D. Leporini, Competition of the connectivity with the local and the global order in polymer melts and crystals, J. Chem. Phys. 139 (2013) 184501.

[35] I. W. Hamley, Introduction to Soft Matter: Synthetic and Biological Self-Assembling Materials, Revised Edition, John Wiley & Sons, Chichester, 2007.

[36] H. Shi, Y. Zhao, X. Dong, Y. Zhou, D. Wang, Frustrated crystallisation and hierarchical self-assembly behaviour of comblike polymers, Chem. Soc. Rev. 42 (2013) 2075–2099.

[37] J. P. K. Doye, A. A. Louis, I.-C. Lin, L. R. Allen, E. G. Noya, A. W. Wilber, H. C. Kok, R. Lyus, Controlling crystallization and its absence: proteins, colloids and patchy models, Phys. Chem. Chem. Phys. 9 (2007) 2197–2205.

[38] R. Mauri, D. Leporini, Violation of the fluctuation-dissipation theorem in confined driven colloids, Europhys. Lett. 76 (2006) 1022–1028.

[39] G. S. Grest, K. Kremer, Molecular dynamics simulation for polymers in the presence of a heat bath, Phys. Rev. A 33 (1986) 3628–3631.

[40] F. Puosi, D. Leporini, Scaling between relaxation, transport, and caged dynamics in polymers: From cage restructuring to diffusion, J.Phys. Chem. B 115 (2011) 14046–14051.

[41] A. Ottochian, D. Leporini, Scaling between structural relaxation and caged dynamics in $ca_{0.4}k_{0.6}(no_3)_{1.4}$ and glycerol: free volume, time scales and implications for the pressure-energy correlations, Philosophical Magazine 91 (2011) 1786–1795.

[42] A. Barbieri, G. Gorini, D. Leporini, Role of the density in the crossover region of o-terphenyl and poly(vinyl acetate), Phys. Rev. E 69 (2004) 061509.

[43] L. Alessi, L. Andreozzi, M. Faetti, D. Leporini, Anisotropic jump model of the rotational dynamics in glasses, J.Chem.Phys. 114 (2001) 3631–3639.

[44] D. Leporini, Relationship between a nonlinear response and relaxation induced by colored noise, Physical Review A 49 (1994) 992–1014.

[45] L. Andreozzi, M. Faetti, M. Giordano, D. Leporini, Scaling between the rotational diffusion of tracers and the relaxation of polymers and glass formers, J. Phys.: Condens. Matter 11 (1999) A131–A137.

[46] S. Plimpton, Fast parallel algorithms for short-range molecular dynamics, J. Comput. Phys. 117 (1995) 1–19.

[47] M. Doi, S. F. Edwards, The Theory of Polymer Dynamics, Clarendon Press, 1988.

[48] J. P. Hansen, I. R. McDonald, Theory of Simple Liquids, 3rd Ed., Academic Press, 2006.

[49] M. Kröger, Simple models for complex nonequilibrium fluids, Phys. Rep. 390 (2004) 453–551.

[50] J. Wedekind, R. Strey, D. Reguera, New method to analyze simulations of activated processes, J. Chem. Phys. 126 (2007) 134103.

[51] P. Yi, G. C. Rutledge, Molecular simulation of crystal nucleation in n-octane melts, J. Chem. Phys. 131 (2009) 134902.

[52] P. Yi, G. C. Rutledge, Molecular simulation of bundle-like crystal nucleation from n-eicosane melts, J. Chem. Phys. 135 (2011)

024903.

[53] J. Baschnagel, F. Varnik, Computer simulations of supercooled polymer melts in the bulk and in confined geometry, J. Phys.: Condens. Matter 17 (2005) R851–R953.

[54] M. D. Rintoul, S. Torquato, Computer simulations of dense hardsphere systems, J. Chem. Phys. 105 (1996) 9258–9265.

[55] P. Richard, L. Oger, J. Troadec, A. Gervois, Geometrical characterization of hard-sphere system, Phys. Rev. E 60 (1999) 4551.